Nucleation and Oriented Growth of Aromatic Crystals on Friction-Transferred Poly(tetrafluoroethylene) Layers

P. Damman,*,† M. Dosière,† M. Brunel,‡ and J. C. Wittmann§

Laboratoire de Physico-Chimie des Polymères, Université de Mons-Hainaut, Place du Parc, 20, B-7000 Mons, Belgium, Laboratoire de Cristallographie du CNRS, Avenue des Martyrs, 25, F-38000 Grenoble, France, and Institut Charles Sadron, rue de Boussingault, 6, F-67083 Strasbourg, France

Received April 9, 1996[⊗]

Abstract: The oriented growth of *p*-nitroaniline and hydroquinone deposited from the vapor phase on monooriented thin films of poly(tetrafluoroethylene) (PTFE) prepared by friction transfer is investigated by grazing incidence X-ray diffraction and polarized FTIR spectroscopy. Due to the formation of two-dimensional hydrogen-bonded networks, both aromatic compounds crystallize with a layered structure. *p*-Nitroaniline is found to contact the $(100)_{PTFE}$ surface with its $(101)_{PNA}$ crystallographic plane which is parallel to the hydrogen-bonded sheet. A similar PTFE/hydrogen-bonded sheet interface was never observed for γ-hydroquinone crystals vacuum deposited under similar experimental conditions. In fact, hydroquinone orients on PTFE with a $(110)_{HYD}$ or $(1\bar{1}0)_{HYD}$ contact plane. Reconstruction of the PTFE substrate at the substrate/deposit interface is invoked as a tentative explanation of the difference in orientational behavior of these two organic compounds.

Introduction

Molecular thin layers not only exhibit interesting fundamental properties but are also very promising candidates for a variety of applications ranging from sensors to electroluminescent diodes, displays, or nonlinear optical devices. It is therefore of prime importance to have strict control over the growth and orientation of these layers. Since heterogeneous nucleation on foreign surfaces is energetically more favorable than homogeneous nucleation, the layer orientation, and to some extent the layer structure, can be efficiently monitored by tuning the interfacial interactions with a selected substrate, i.e., by epitaxy. The oriented growth of both molecular and macromolecular crystals has been achieved on a variety of substrates including ionic substrates,[1] organic crystals,[2,3] Langmuir−Blodgett layers,[4] and oriented polymer thin films.[5] It was shown that lattice matching is often a key feature of the orientation process. Ward and co-workers[2] demonstrated further that crystallographically well-defined ledges of the substrate may act as preferentiel nucleation sites through a mechanism which rests not only on lattice matching but also on a good matching of the ledge and the growing nuclei geometry.

Oriented polytetrafluoroethylene (PTFE) thin layers obtained by the friction transfer method have a single-crystal-like texture over a large surface (several cm^2), the polymer chains being extended along the friction direction. They are highly efficient in inducing the orientation of low and high molecular weight liquid crystalline and crystalline materials.[6] For example, the crystallization of *p*-nitrophenol (PNP)[7] and sesquithiophene (6T)[8] onto PTFE yields thin layers with a unique orientation. For epitaxially grown 6T layers, the *molecular axis* is oriented parallel to the PTFE chain axis; as a result, two symmetrical orientations of the 6T monoclinic unit cell with respect to the substrate are obtained. For PNP, the β structure grown on PTFE is made of regularly stacked planar chains or ribbons of hydrogen-bonded molecules which lie parallel to the substrate surface. In addition, the PNP molecular ribbon axis and the PTFE chain axis are parallel. In both cases, the epitaxial growth rests on a proper deposit/substrate interlocking and a nearly perfect lattice matching.

As part of an ongoing analysis of the versatility of PTFE layers as orienting substrates, the present paper describes the oriented growth of two other aromatic compounds, *p*-nitroaniline (PNA) and hydroquinone (HYD). Contrary to PNP, they do not form *hydrogen-bonded chains*, but *hydrogen-bonded sheets*. The present study demonstrates that the growth of PNA and HYD on PTFE leads to very different crystal orientations, despite the fact that their crystalline structures are very similar.

Experimental Section

Materials. Hydroquinone (T_m = 174 °C) and *p*-nitroaniline (T_m = 149 °C) were both purchased from Aldrich Chemical Company and were used without further purification. The PTFE substrates are prepared according to the method described in previous publications,[6] by sliding at constant pressure and temperature a PTFE rod against glass slides or the silicon wafers used for the grazing incidence X-ray diffraction (GIXD) experiments. The deposition of the aromatic crystals on the PTFE substrates is achieved by sublimation under vacuum ($\sim 10^{-4}$ Pa). The temperature of the source material (T_C) is controlled by immersing the flat bottom of the pyrex tube in an oil thermostat,

† Université de Mons-Hainaut.
‡ Laboratoire de Cristallographie du CNRS.
§ Institut Charles Sadron.
⊗ Abstract published in *Advance ACS Abstracts,* April 1, 1997.

(1) Swei, G. *Encycl. Polymer Sci. Eng.* **1986**, *6*, 209.
(2) (a) Carter, P. W.; Ward, M. D. *J. Am. Chem. Soc.* **1993**, *115*, 11521. (b) Bonafede, S. J.; Ward, M. D. *J. Am. Chem. Soc.* **1995**, *117*, 7853.
(3) Wittmann, J. C.; Lotz, B. *Electron crystallography of organic molecules;* Fryer, J. F., Dorset, D. L., Eds.; Kluwer: The Netherlands, 1990; pp 241−254.
(4) Landau, L. M.; Grayer, S.; Levanon, M.; Leiserowitz, L.; Lahav, M.; Sagiv, J. *J. Am. Chem. Soc.* **1989**, *111*, 1436.
(5) Kawaguchi, A.; Okihara, T.; Katayama, K. *J. Cryst. Growth* **1990**, *99*, 1028.
(6) (a) Wittmann, J. C.; Smith, P. *Nature* **1990**, *352*, 414. (b) Hansma, H.; Motamedi, F.; Smith, P.; Hansma, P.; Wittmann, J. C. *Polymer* **1992**, *33*, 647. (c) Dietz, P.; Hansma, P. K.; Ihn, K. J.; Motamedi, F.; Smith, P. *J. Mater. Sci.* **1993**, *28*, 1372. (d) Meyer, S. Ph.D. Thesis, University of Strasbourg, 1995.
(7) Damman, P.; Dosière, M.; Smith, P.; Wittmann, J. C. *J. Am. Chem. Soc.* **1995**, *117*, 1117.
(8) Lang, P.; Valat, P.; Horowitz, G.; Garnier, F.; Yassar, A.;Wittmann, J. C.; Lotz, B.; Meyer, S. *J. Chem. Phys.* **1995**, *92*, 963.

S0002-7863(96)01173-0 CCC: $14.00

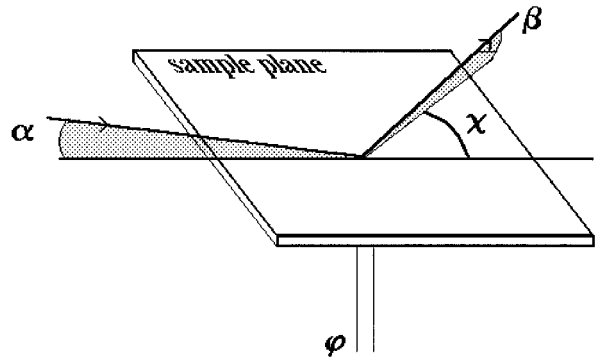

Figure 1. Schematic representation of the angle settings used for the GIXD experiments.

while the PTFE substrate is held at 15 °C by using a water-cooled finger. At this temperature, the PTFE layer is in its low-temperature crystal form with a triclinic (nearly hexagonal) unit cell[9] ($a = b =$ 0.56 nm, $c = 1.68$ nm, $\gamma = 119.5°$). For the FTIR measurements, the PTFE/deposit bilayers are floated off on water and picked up on copper grids.

Optical Microscopy. The microscopical observations were carried out in polarized light with a Leitz Ortholux microscope fitted with an Orthomat photographic system and in phase contrast with a Leitz Laborlux microscope.

Grazing Incidence X-ray Diffraction. The GIXD measurements used to determine the crystal structure, and orientation of the deposited aromatic layers are performed using a Rigaku Denki generator with a rotating anode (12 kW) fitted with a graphite monochromator ($\lambda =$ 0.154 18 nm). The horizontal and vertical divergences of the incident beam are limited by two tantalum slits. Additionally, soller slits are used to perform accurate measurements of the peak positions. The scattering measurements are made using a modified four circles diffractometer with the sample held vertical and a NaI detector. A symmetrical geometry ($\alpha = \beta$) with an incidence angle of 0.5° with respect to the sample plane is used (Figure 1). Since this incidence angle is well above the critical angle (about 0.1° for such organic compounds), the total thickness of the deposited layer contributes to the diffraction.[10] Also, since the detector moves nearly in the plane of the sample ($\beta \cong 0°$), only the reciprocal plane corresponding to the sample plane is investigated, the diffraction angle 2θ being equal to χ. The (220) reflection due to the silicon wafer support is used as an internal calibration standard. To determine the azimuthal orientation of the layer with respect to the PTFE substrate, the angular position φ^* of each reflection with respect to the PTFE chain axis direction was measured. φ^* is given by $\varphi^* = \pi/2 + \theta - \varphi$, where θ and φ are the diffraction and the rotation angles in the sample plane, respectively.

Comparison of the observed and calculated values of φ^* helps to establish the crystallographic relationship between the substrate and the deposited organic layer.

FTIR Spectroscopy. FTIR spectra were recorded in a manner similar to that described for *p*-nitrophenol.[7] A Bruker IFS113v FTIR spectrometer fitted with a microscope working either in reflection or transmission mode is used. The diameter of the observed area is close to 100 μm. At least 500 interferograms with a resolution of 2 cm^{-1} are collected. The assignement of PNA and HYD IR bands is made by taking into account the results obtained on various substituted aromatic molecules[11] and comparing the experimental observations (frequency and polarization) with the results of normal mode analyses performed with the Cerius[2] molecular-modeling software package (Molecular Simulations, Inc., Cambridge, UK; MOPAC package).

Results

Nucleation and Growth of *p*-Nitroaniline and Hydroquinone Crystalline Layers on PTFE Substrates. Deposition of *p*-nitroaniline (PNA) and hydroquinone (HYD) onto PTFE substrates is performed from the vapor phase at sublimation temperatures ranging from 50 °C up to the melting temperatures of the compounds. The temperature difference between the source material and the substrate determines the supersaturation of the vapor and thus the free energy of crystallization. When deposited on PTFE substrates from highly supersaturated vapors, both aromatic compounds form uniform and birefringent layers (cf. Figure 2) which show total extinction or a maximum of birefringence when the underlying PTFE chains (parallel to the friction direction) are oriented parallel or at 45° to the polarizers, respectively. Closer examination in phase contrast microscopy (Figure 3) reveals that the layers are in fact made of uniformly oriented single crystals a few micrometers in size. Lowering the supersaturation of the organic vapor increases the free energy of nucleation and thus decreases the density of nuclei; as shown in Figures 4 and 5, much larger PNA and HYD single crystals are therefore obtained. The PNA crystals grown on PTFE substrates exhibit a rectangular shape very different from the needle shape usually obtained when PNA is sublimed or when aqueous PNA solutions are slowly evaporated.[12] Similarly, the small rectangular HYD crystals formed on the PTFE differ from the very thin platelets grown on bare glass, which contact the surface with the $(100)_{HYD}$ H-bonded layer.[13,14] Finally, as is readily apparent in Figure 6, extensive row nucleation along prominent steps or ridges running parallel to the chain axis direction of the PTFE substrate[6] occurs under these growth conditions. These observations highlight the strong influence

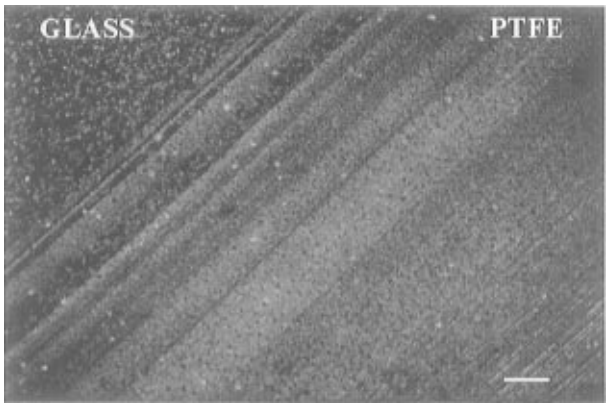

Figure 2. Polarized light optical micrograph of a PNA layer deposited under vacuum on the $(100)_{PTFE}$ substrate surface: source temperature 150 °C, substrate temperature 15 °C (scale bar 10 μm).

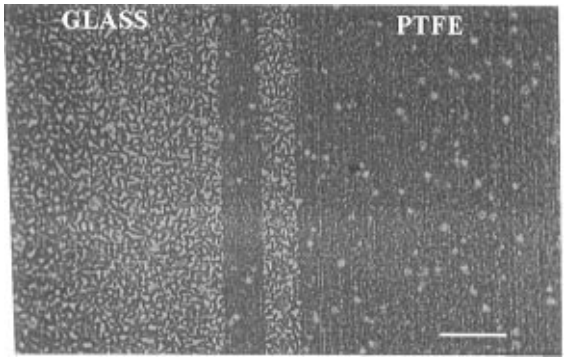

Figure 3. Phase contrast optical micrograph of a HYD layer deposited on PTFE: source temperature 175 °C, substrate temperature 15 °C (scale bar 10 μm).

(9) Bunn, C. W.; Howells, E. R. *Nature* **1954**, *174*, 549.
(10) Brunel, M.; de Bergevin, F. *Acta Crystallogr.* **1986**, *A42*, 299.
(11) (a) Garrigou-Lagrange, C.; Lebas, J. M.; Josien, M. L. *Spectrochim. Acta* **1958**, *12*, 305. (b) Green, J. H. S. *Spectrochim. Acta* **1970**, *26A*, 1503. (c) Stojiljkovic, A.; Whiffen, D. H. *Spectrochim. Acta* **1958**, *12*, 57.
(12) (a) Donohue, J.; Trueblood, K. N. *Acta Crystallogr.* **1956**, *9*, 960. (b) Trueblood, K. N.; Goldish, E.; Donohue, J. *Acta Crystallogr.* **1961**, *14*, 1009.
(13) Caspari *J. Chem. Soc.* **1927**, *131*, 1093.
(14) Maartmann-Moe, K. *Acta Crystallogr.* **1966**, *21*, 979.

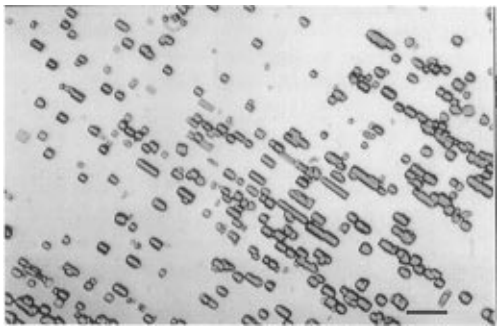

Figure 4. Optical micrograph of PNA single crystals grown on a monooriented PTFE substrate: source temperature 50 °C, substrate temperature 15 °C (scale bar 10 μm).

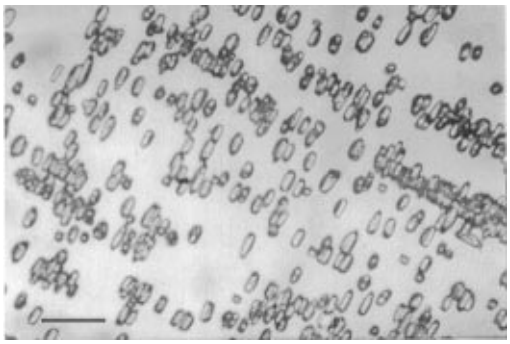

Figure 5. Optical micrograph of HYD single crystals grown on PTFE: source temperature 70 °C, substrate temperature 15 °C (scale bar 10 μm).

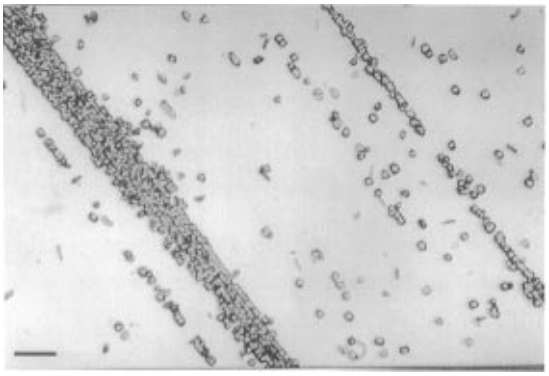

Figure 6. Optical micrograph showing the enhanced nucleation of PNA crystals along steps or grooves runing parallel to the PTFE sliding direction (scale bar 10 μm).

of the substrate surface topography and defects on the nucleation process, as reported and discussed recently by Ward et al.[2]

Obviously, PTFE substrates dramatically increase the density of nuclei in comparison with glass and are able to induce the oriented growth of both PNA and HYD crystals, the sizes of which depend on the degree of supersaturation. Although the PNA and HYD layer morphologies are nearly identical, analysis of the molecular orientation by X-ray diffraction and FTIR spectroscopy reveals that their crystallographic relationships with the PTFE substrates are quite different.

Molecular Orientation on PTFE Substrates: X-ray Diffraction. In view of the high vapor pressure of both organic compounds, grazing incidence X-ray diffraction (GIXD) was preferred to electron diffraction to determine the crystal orientation in the thin films.

***p*-Nitroaniline.** The crystal structure of PNA[12] is based on a monoclinic unit cell containing four molecules (a = 1.234 nm, b = 0.607 nm, c = 0.863 nm, and β = 91.45°; $P2_1/n$ symmetry). Each amino group forms two hydrogen bonds with

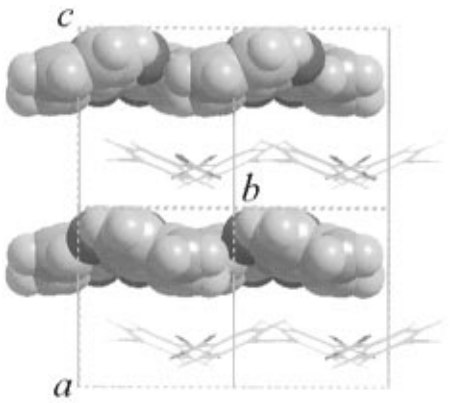

Figure 7. Computer-generated molecular model of $(101)_{PNA}$ hydrogen-bonded PNA sheets.

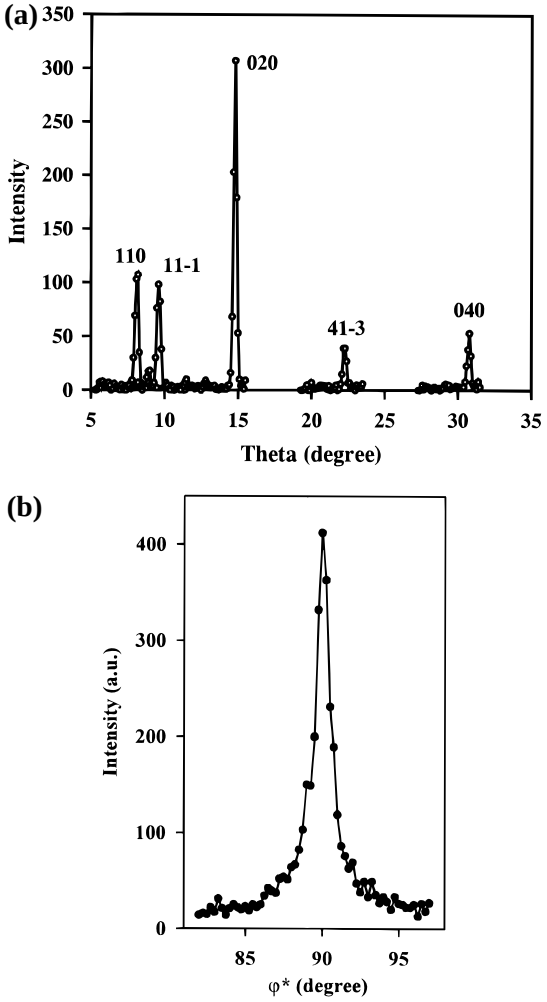

Figure 8. (a) GIXD spectra (θ scans) of an oriented PNA thin film; the Miller indices of the observed reflections are as indicated. (b) φ* scan of the (020) reflection.

the nitro groups of neighboring molecules, thus giving rise to hydrogen-bonded sheets parallel to the $(101)_{PNA}$ crystallographic plane (Figure 7).

The GIXD spectra of oriented PNA layers are given in Figure 8a (the φ scans are omitted for clarity). Figure 8b shows a φ* scan for the PNA (020) reflection. The half-width at mid-height of only 1° illustrates the very high degree of orientation of PNA induced by the PTFE substrate. The indexation of the various diffraction peaks, together with their observed and calculated angular positions φ* with respect to the PTFE chain axis direction, is reported in Table 1. All reflections can be indexed

Table 1. X-ray Diffraction Data of PNA Crystals Grown on PTFE

hkl	θ (deg)	φ^*_{calcd} (deg)	φ^*_{obsd} (deg)
$11\bar{0}$	8.1	68	69
$11\bar{1}$	9.6	51	52
$02\bar{0}$	14.7	90	93
$41\bar{3}$	22.2	20	19
040	30.7	90	93

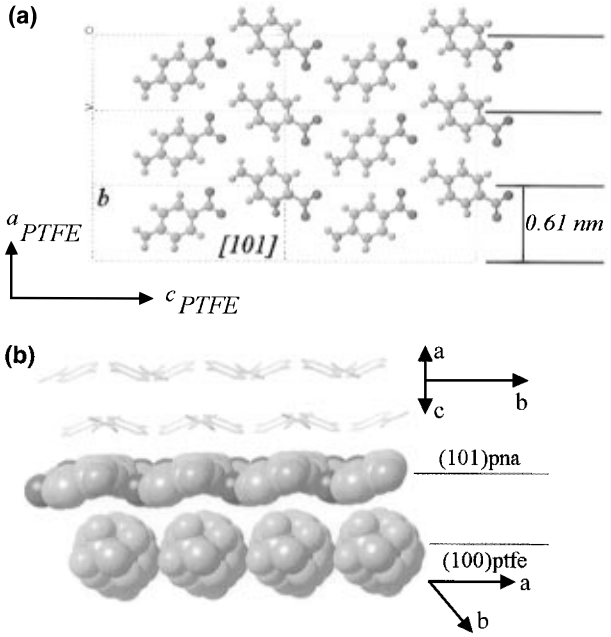

Figure 9. Molecular models of (a) the $(101)_{PNA}$ contact plane and (b) the PTFE/PNA interface projected along the PTFE chain axis.

on the basis of the known monoclinic unit cell of PNA. These data indicate that the PNA crystals contact the $(100)_{PTFE}$ surface with the densely packed $(101)_{PNA}$ plane, which corresponds actually to the hydrogen-bonded molecular sheet. Moreover, the angular positions of the diffraction peaks show that the PNA [101] and [010] axes are parallel and perpendicular to the PTFE chain axis, respectively. Note that the polar axis of the PNA molecule lies in the $(101)_{PNA}$ contact plane and makes an angle of $\pm 27.8°$ with respect to $[101]_{PNA}$.

The PNA/PTFE crystallographic relationships can be summarized as follows:

$$(101)_{PNA}//(100)_{PTFE}$$

$$[101]_{PNA}//[001]_{PTFE} \text{ or else } [010]_{PNA}//[100]_{PTFE}$$

A molecular model of the $(101)_{PNA}$ plane and a side-view model of the PNA/PTFE interface based on these crystallographic relationships are shown in Figure 9.

Hydroquinone. HYD exists in two different modifications: hexagonal α ($a = 2.21$ nm, $c = 0.56$ nm; P_3 or P_{-3} symmetry)[13] and monoclinic γ modification[14] ($P2_1/c$ symmetry, 4 molecules per unit cell) of parameters $a = 0.81$ nm, $b = 0.52$ nm, $c = 1.32$ nm, $\beta = 107°$. The latter is usually observed for crystals grown by sublimation; it bears close resemblance with the PNA crystal structure in that the HYD molecules are also arranged in densely packed hydrogen-bonded sheets (Figure 10).

The GIXD results (Figure 11a) indicate that only the γ form of hydroquinone crystallizes on PTFE. The indexation of the various diffraction peaks is given in Table 2. The observed reflections belong to the zero and first layer lines of a $[1\bar{2}0]$ zone axis diffraction pattern (cf. Figure 11b). The HYD crystals contact the $(100)_{PTFE}$ substrate with their $(110)_{HYD}$ or $(1\bar{1}0)_{HYD}$

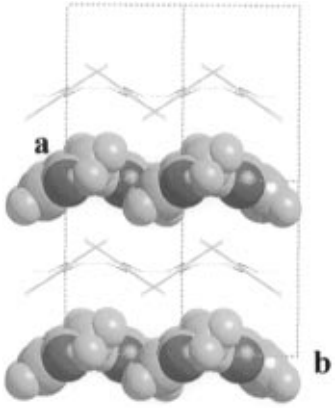

Figure 10. Molecular model of the $(100)_{HYD}$ hydrogen bonded sheet in the γ crystal structure of HYD.

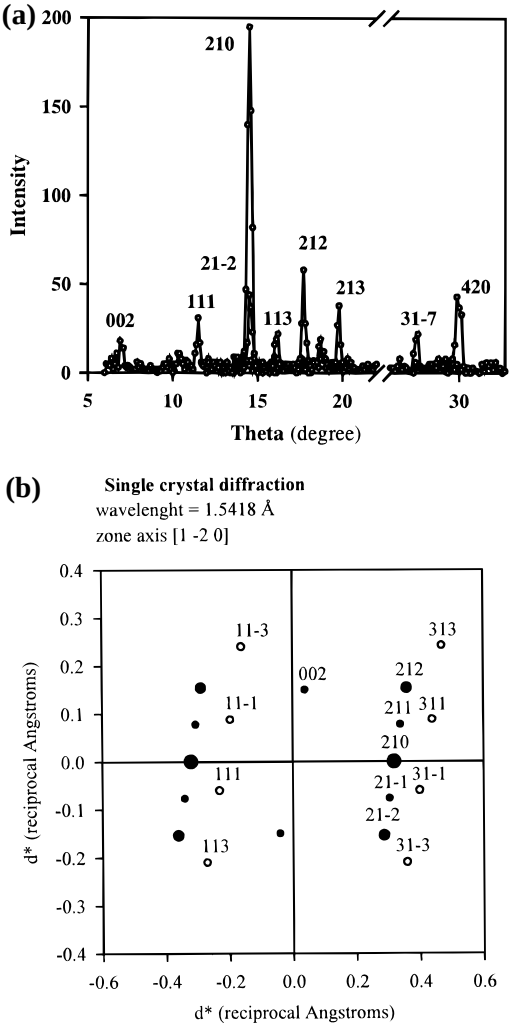

Figure 11. (a) GIXD spectra (θ scans) of a HYD thin film oriented on PTFE. (b) Simulation of a single crystal diffraction pattern of HYD: $[1\bar{2}0]$ zone axis (° first layer, ● second layer).

planes, the $[001]_{HYD}$ zone axis lying parallel to the PTFE chain axis (Figure 12a). The substrate/deposit crystallographic relationships deduced from the diffraction data are therefore

$$(1\bar{1}0)_{HYD}//(100)_{PTFE}$$

$$[001]_{HYD}//[001]_{PTFE}$$

Contrary to epitaxially grown PNA layers, *the $(100)_{HYD}$ hydrogen-bonded sheets are not parallel to the PTFE substrate*

Table 2. X-ray Diffraction Data of a HYD-Oriented Thin Film

hkl	θ (deg)	φ^*_{calcd} (deg)	φ^*_{obsd} (deg)
002	6.9	14	14
111	11.4	72	72
210	14.4	90	92
21$\bar{2}$	14.4	61	62
113	16.0	50	50
21$\bar{2}$	17.6	68	68
31$\bar{2}$	18.6	68	68
21$\bar{3}$	19.7	57	59
31$\bar{7}$	28.1	25	-27
420	29.9	90	92

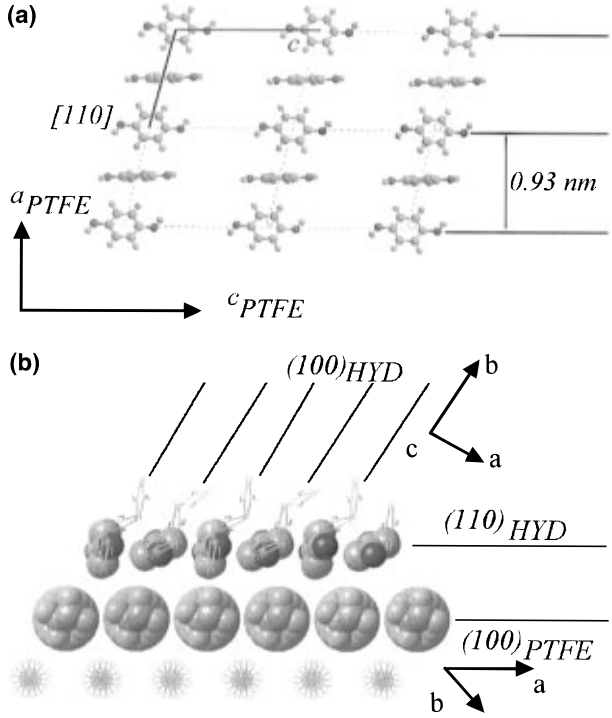

Figure 12. Molecular model of: (a) the (110) contact plane and (b) the HYD/PTFE interface viewed down the PTFE chain axis.

surface but are inclined at an angle of ~55° to the substrate surface, which is also the plane of the thin film (Figure 12b).

Molecular Orientation on PTFE Substrates: FTIR Spectroscopy. The *p*-nitroaniline and hydroquinone molecules possess the symmetry elements of the C_{2v} and C_{2h} point groups, respectively. For such *p*-disubstituted aromatic compounds, the transition moments associated with the normal modes are parallel either to the aromatic ring (in plane modes) or to the out-of-plane axis. The transition moments associated with the normal modes A_1, B_1, and B_2 for PNA (C_{2v}) or $B_u(z)$, $B_u(y)$, and A_u for HYD (C_{2h}) are aligned in both cases with the C1−C4 direction, the in-plane axis normal to the C1−C4 axis and the out-of-plane axis, respectively. Regarding the crystal vibrations, they are derived from the molecular vibrations and the molecular orientation in the unit cell, as indicated in Table 3. For the PNA crystals (space group C_{2h}^5), the site symmetry corresponds to the C_1 point group for which all the molecular vibrations may be IR active (cf., the correlation diagram given in Table 3). Each molecular vibration is split into two crystal modes having their transition moments either parallel to the *b* axis (A_u modes) or lying in the *ac* crystallographic plane (B_u modes). Similarly, HYD crystals have the symmetry of the C_{2h}^5 space group, the site symmetry group being C_i; the molecular vibrations are again split into two crystal modes A_u and B_u having their transition moments either parallel to the *b* axis or in the *ac* plane, respectively.

Table 3. Correlation Diagram of PNA

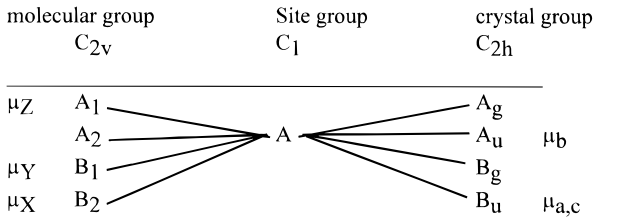

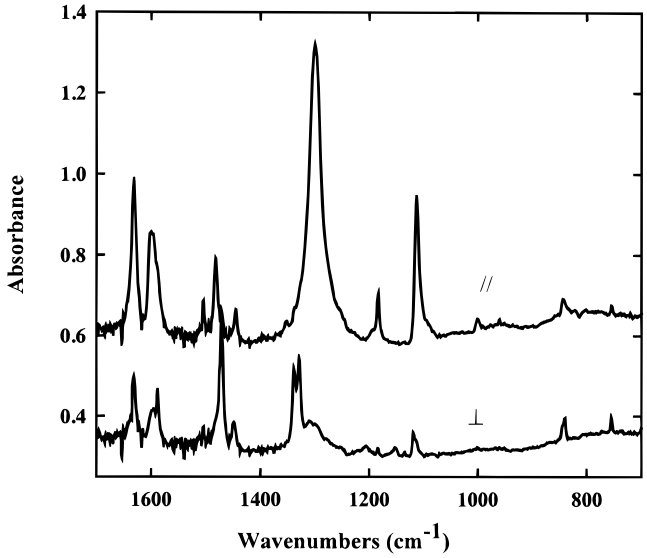

Figure 13. Polarized FTIR spectra of a thin film of PNA oriented on PTFE.

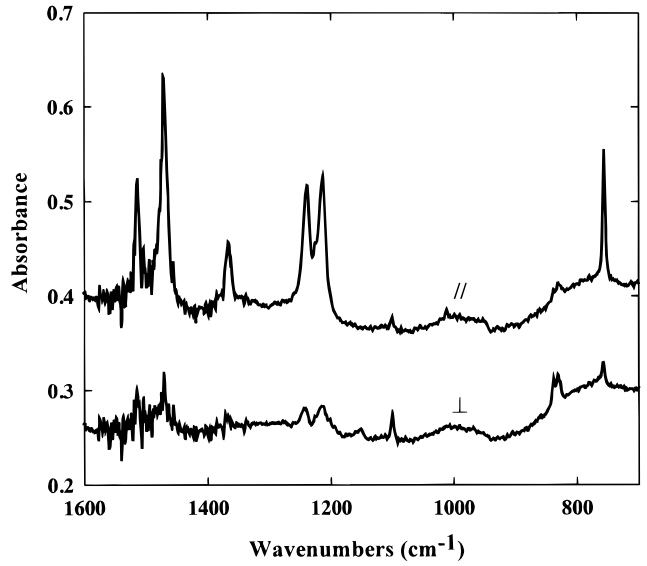

Figure 14. Polarized FTIR spectra obtained for a thin film of HYD oriented on PTFE.

The FTIR spectra of PNA and HYD crystals recorded with the polarization either parallel or perpendicular to the PTFE chain axis (sliding direction) are shown in Figures 13 and 14, and the corresponding data (wavenumbers of the vibrations, dichroism, and attribution of the IR bands) are collected in Tables 4 and 5, respectively.

The polarized FTIR measurements are fully consistent with an orientation of the PNA crystals involving a $(101)_{PNA}$ contact plane with the PTFE substrate. In accordance with the molecular orientation shown in Figure 9a, a strong parallel

Table 4. Wavenumbers, Dichroism, and Attribution of the IR Bands of PNA Crystallized onto PTFE Substrates[a]

wavenumber (cm^{-1})*	dichroism, *R*	attribution, calcd wavenumber (cm^{-1})
w 697	⊥, −	B_2, 680
w 755	⊥, 0.4	B_2, 794
w 840	⊥, 0.2	B_2, 881
w 843	//, --	A_1, 808
w 1001	//, 3.5	A_1, 1002
s 1112	//, 20	A_1 crystal, 1125
vw 1135	−	$^{\beta as}NH_2$ B_1, 1086
w 1152	⊥, 0.2	B_1
m 1183	//, 7	A_1, 1177
w 1205	⊥, 0.4	B_1, 1196
vs 1300	//, 20	A_1, $^{\nu s}NO_2$ crystal
m 1329	⊥, −	B_1, 1279
s 1471	⊥, 0.1	$^{\nu as}NO_2$
m 1481	//, 11	A_1, 1498
m 1600	//, 3.5	$^{\nu s}NO_2$ A_1, 1611
s 1633	//, 2.4	$^{\beta s}NH_2$ A_1, 1542
s 3354	//, 10	$^{\nu s}NH_2$, 3155
w 3480	⊥, 0.3	$^{\nu as}NH_2$, 3144

[a] The // and ⊥ refer to spectra recorded with an IR beam polarized parallel and perpendicular to the PTFE chain axis, respectively). The wavenumbers are calculated with Cerius[2] (MOPAC package). [b] The vw, w, m, s, and vs correspond to very weak, weak, medium, strong, and very strong intensities.

Table 5. Wavenumbers, Dichroism, and Attribution of the IR Bands of HYD Crystallized onto PTFE Substrates[a]

wavenumber (cm^{-1})	dichroism, *R*	attribution, calcd wavenumber (cm^{-1})
vs 758	//, 7	B_u (*z*), 765
vw 830	⊥, 0.3	A_u (*x*), 868
vw 1012	//, −	B_u (*z*), 988
m 1100	⊥, 0.5	B_u (*y*), 1036
vs 1213	//, 6	B_u (*z*) β_{OH}, 1189
vs 1237	//, 6	B_u (*z*), 1232
m 1365	//, 5	B_u (*z*) β_{OH}, 1309
vs 1469	//, 4.5	B_u (*z*) β_{OH}, 1470
m 1513	//, 4	B_u (*z*), 1502
s 3322	⊥, −	B_u crystal b, ν_{OH}
s 3372	//, −	B_u crystal c, ν_{OH}

[a] Cf., legend Table 4.

dichroism is indeed observed for all the A_1 normal modes while B_1 and B_2 modes are polarized perpendicular to the PTFE chain axis (Figure 13, Table 4). Moreover, the transition moments of both crystal vibrations associated with these A_1 molecular modes correspond to (i) the intercept of the $(101)_{PNA}$ plane with the *ac* crystallographic plane (parallel to the PTFE chain axis in the proposed orientation) and (ii) the *b* axis. Using an angle of 28° between the C1−C4 axis and the [101] zone axis, an ideal dichroic ratio *R* of 3.9 is derived. Deviations from this calculated value may be related to a crystal splitting due to hydrogen bonding along the $[101]_{PNA}$ axis (values of *R* as large as 20 are observed in Figure 13).

For HYD, a strong parallel dichroism is observed for the B_u-(*z*) normal modes, the B_u(*y*) and A_u vibrations being polarized perpendicular to the PTFE chain axis (Table 5). This indicates that the molecular C1−C4 axis (parallel to the $[001]_{HYD}$ axis) is oriented along the PTFE chain axis. This result is fully consistent with the orientation deduced from the GIXD measurements (Figure 12a). Moreover, in such hydrogen-bonded crystals, the OH vibrations are obviously sensitive to intermolecular interactions. As already mentionned, HYD molecules form a layered structure made of H-bonded sheets lying parallel to the *bc* crystallographic plane.[14] Due to the crystal field, the stretching OH band is therefore split into two components having their transition moments parallel to either the *c* or the *b* axis. They correspond to the two bands observed at 3372 and 3322 cm^{-1} which are indeed polarized parallel and perpendicular to the PTFE chain axis, respectively.

Discussion

The major result of the present work is that although *p*-nitroaniline and hydroquinone have very similar crystalline structures (see Figures 7 and 10), they behave differently in the presence of PTFE substrates. Apparently, minute changes in the crystal structure are able to induce important changes in the polymer/deposit crystallographic relationships. PNA contacts the PTFE substrate with its $(101)_{PNA}$ H-bonded plane. The PNA planar molecules lie parallel to either the (312) or the $(3\bar{1}2)$ crystallographic planes and are thus symmetrically inclined by ∼28° with respect to the $(101)_{PNA}$ contact plane. The H-bonded sheet is therefore slightly corrugated with a characteristic distance of 0.607 nm (*b* parameter of the PNA unit cell; Figure 9b) between corrugations. Adequate interlocking of the substrate and the deposit contact planes leads to a lattice mismatch of $\Delta = (b_{PNA} - a_{PTFE})/a_{PTFE} \cong +9\%$.

A similar pattern of interaction between HYD and PTFE would appear as a likely possibility. Indeed, a pure geometric fit of the densely packed $(100)_{HYD}$ H-bonded plane with the substrate, as observed for PNA, would lead to a lattice mismatch of $\Delta \cong -7\%$ (note for future reference the negative sign). However, this orientation is not observed. To the contrary, hydroquinone crystals grow with their H-bonded sheets inclined at 55°, i.e., with their $(110)_{HYD}$ or $(1\bar{1}0)_{HYD}$ plane in contact with the $(100)_{PTFE}$ surface. The HYD periodicity, which corresponds in this case to d_{210}, is equal to 0.305 nm, and the substrate/deposit disregistry is given by the relation $\Delta = (2d^{210}_{HYD} - a_{PTFE})/a_{PTFE}$, is again close to +9%.

Such a difference in growth geometry and orientation may have several origins: formation of a transient layer of an unstable polymorphic form at the interface which transform into the observed HYD γ phase (a phenomenon observed for instance for polyethylene epitaxially grown on various organic or inorganic substrates[15]), kinetically favored crystal growth direction leading to a macroscopic orientation in the bulk of the film different from that at the interface, or interfacial reconstruction process of low energetic cost of the deposit or the substrate. The role of the interfacial energetics on the epitaxial growth of several organic overlayers on graphite substrates were recently discussed by Ward and co-workers.[16]

Regarding possible interfacial reconstruction, a preliminary molecular-modeling study shows that a small *increase* of the PTFE interchain distance (from 0.56 to 0.607 nm) to accommodate the PNA periodicity is possible at a low energetic cost (ΔE = 0.5 kcal/mol for one unit cell).[17] For HYD on the contrary, a similar reconstruction of the PTFE substrate to accommodate the $(100)_{HYD}$ H-bonded plane thus leading to the same crystal orientation is highly improbable since it would require a *decrease* of the PTFE interchain distance from 0.56 to 0.52 nm, which in terms of energy is of high cost (ΔE = 14.2 kcal/mol). Therefore, despite a less favorable substrate/deposit lattice matching, a different crystal orientation which implies a substrate reconstruction identical to the one described for PNA (same increase from 0.56 to 0.61 nm of the PTFE interchain distance) is observed. We note that a similar mechanism is invoked by Ward et al. to explain the growth of

(15) Wittmann, J. C.; Lotz, B. *Polymer* **1989**, *30*, 27.
(16) Hillier, A. C.; Ward, M. D. *Phys. Rev. B* **1997**, accepted for publication.
(17) Damman, P., manuscript in preparation.

$(ET)_2I_3$ crystals with a (011) orientation on highly oriented pyrolytic graphite (ET refers to bis(ethylenedithio)tetrathiafulvalene).[16]

In conclusion, both *p*-nitroaniline and hydroquinone crystallize epitaxially on PTFE substrates when deposited from the vapor phase. However, in spite of obvious similarities in their crystalline structures, the resulting orientation of these two aromatic compounds are very different: the PNA crystals contact the PTFE surface with the hydrogen-bonded sheet while the HYD contact plane corresponds to the $(110)_{HYD}$ plane 55° apart from the hydrogen-bonded layer. In both cases, an acceptable substrate/deposit lattice matching is observed. The proposed origin of the change in orientation is based on an energetically feasible substrate reconstruction. However, this assumption needs be further supported by different and more detailed data on the epitaxial growth of other hydrogen-bonded, self-assembling systems.

Acknowledgment. P. Damman is a Research Associate of the Belgian National Funds for Scientific Research. The authors gratefully acknowledge the support of the Belgian National Funds for Scientific Research (FNRS) and the CNRS (France). The authors also acknowledge Dr. B. Lotz (Institut Charles Sadron) and Prof. M. D. Ward (University of Minnesota, Department of Chemical Engineering and Material Science) for helpful discussions.

JA961173K